- Technical Paper -

NONLINEAR FINITE ELEMENT ANALYSIS OF RC CANTILIVER STRUCTURAL WALLS UNDER LATERAL LOADING

Rafik TALEB[*1], Susumu KONO[*2] and Masanobu SAKASHITA[*3]

ABSTRACT

The aim of this paper is to present nonlinear finite element (FE) analyses results on four 40%-scale cantilever type reinforced concrete (RC) structural walls with and without boundary columns with different amount of boundary region shear reinforcement. FE model was built in order to simulate the load-deformation relations as well as cracking and damage patterns. The model is able to predict yielding, peak load and damage pattern with reasonably good accuracy. The model is capable of predicting the ability of boundary columns in reducing damage level.

Keywords: Cantilever RC structural walls, boundary columns, confined regions, nonlinear FE analysis.

1. INTRODUCTION

RC structural walls are frequently used as lateral force-resisting system in building construction because they have sufficient stiffness and strength against damage and collapse. If properly designed, these structural walls can also behave as ductile flexural members. To achieve this goal, the designer should provide adequate strength and deformation capacity. Hence, several experimental and analytical studies were conducted to investigate the behaviour of RC structural walls under lateral loads in order for designers to predict their structural performance when they are subjected to severe seismic excitations [1, 2]. The criteria for the structural performance of a structural wall can be represented by the stiffness, strength and deformation capacity inherent in the structure. These parameters depend on the load history, sectional shape, vertical and horizontal reinforcement, boundary details, moment to shear ratio, axial load, and concrete strength, etc. Beside, predicting the behaviour of RC walls under lateral loads requires enhanced numerical tools that are calibrated using controlled experimental tests. These tools should take into account most of the important factors that could affect the response of RC walls. Hence, modeling of RC walls involves several challenges.

Framed RC structural walls with boundary columns and beams provide strong confinement to wall panels and thus, have substantially higher bending strength and horizontal shear force carrying capacity which enables the wall system to achieve a higher ductile manner and are therefore less susceptible to earthquake damage than walls without boundary elements. Boundary columns can also reduce the development of cracks on the wall and therefore enhance the reparability characteristics compared with RC structural walls without boundary columns. The objective of this study is to presents nonlinear finite element simulation results of four 40%-scale cantilever type structural walls with and without boundary columns and with two levels of the boundary region shear reinforcement in order to simulate the load-deformation relations as well as cracking and damage patterns.

2. EXPERIMENTAL WORK

Experimental studies were conducted on four 40% scale structural walls prepared by changing the configuration of section (barbell-shape and rectangular sections) and the amount of shear reinforcement in confined regions as shown in Fig. 1. The walls were tested under lateral cyclic reversal loading in order to evaluate the effects of boundary region size and their confining shear reinforcement on the seismic performance of structural walls. The experimental work was already reported in [3]. Minimum information is provided in this paper. The total area of wall sections, the area of confined boundary regions and the moment capacity were set equal for all specimens. Geometrical properties and reinforcement amount are summarized in Table 1. Specimens BC40 and BC80 had confined boundary columns and NC40 and NC80 had no boundary columns but confined boundary regions instead with same thickness as for the wall panel. The four specimens had same depth (1750 mm), nearly same total section area (2250 cm^2 for BC's and 2240 cm^2 for NC's) and confined boundary region area (625 cm^2 for BC's and 666 cm^2 for NC's).

*1 Doctoral Student, Dept. of Environmental Science and Engineering, Tokyo Tech, JCI Member
*2 Professor, Materials and Structures Laboratory, Tokyo Tech, JCI Member
*3 Assistant Prof., Dept. of Architecture and Architectural Engineering, Kyoto University, JCI Member

The specimens were casted in two stages, first the foundation beam and second the wall and the loading beam as one part with intentionally roughened surface created at the foundation–wall interface to insure good adherence. Table 2 lists the mechanical properties of concrete and reinforcement. The specimens were tested under cyclic loading. Axial force of 1500 kN was applied constantly by two hydraulic jacks to keep the axial load level of 0.20 for confined region, which is 0.11 for the total area of the section. The lateral load, *Q*, was applied at the center of the top loading beam, which is 3000 mm high from the top of the foundation. Hence, the shear span ratio was 1.71. The shear capacity was set to more than 1.5 times larger than the flexural capacity to insure flexural failure mode.

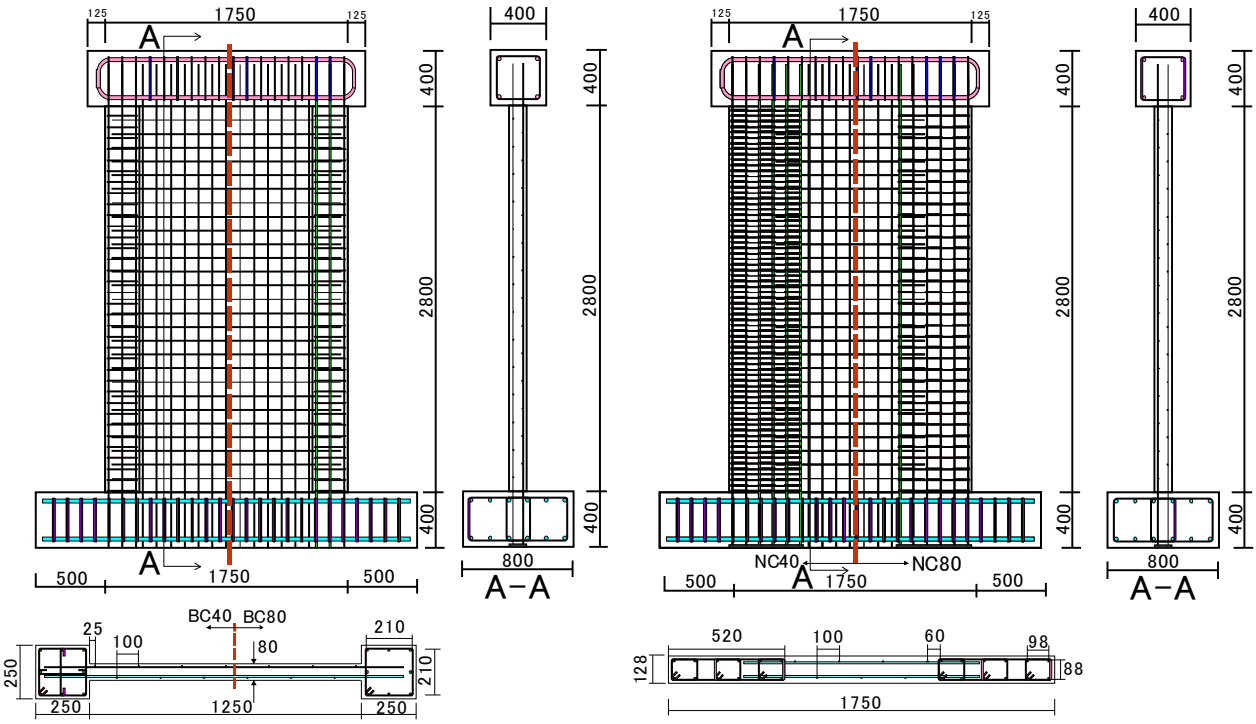

(a) BC40 (left) and BC80 (right) (b) NC40 (left) and NC80 (right)

Fig. 1 Dimensions and reinforcement details of specimens (Unit: mm)

Table 1 Specimens geometry and Reinforcement

Specimen	Width & height (mm)	Confined area			Wall panel	
		Section dimension (mm)	Long. Reinf. (rebar ratio)	Shear reinf. (rebar ratio)	Thickness (mm)	Shear reinf. (rebar ratio)
BC40	1750 2800	250x250	8-D10 (0.91%)	3-D6@40 (0.95%)	80	D6@100 Staggered (0.40%)
BC80				2-D6@80 (0.32%)		
NC40		128x520	12-D10 (1.29%)	4-D6@40 (2.47%)	128	D6@100 Staggered (0.25%)
NC80				4-D6@80 (1.24%)		

Table 2 Materials mechanical properties

Specimen	Concrete			Reinf. bar	Steel		
	Compressive strength (MPa)	Young's modulus (GPa)	Splitting strength (MPa)		Yield strength (MPa)	Young's modulus (GPa)	Tensile strength (MPa)
BC40 BC80	59.5	30.9	5.10	D6	387	189	496
NC40 NC80	52.5	30.1	3.66	D10	377	194	533

Fig. 2 shows the observed lateral load - drift angle relations. The figure shows the characteristic points: cracking, yielding of longitudinal reinforcement, peak load, and ultimate deformation. All specimens generally behaved in a flexural manner by yielding of the longitudinal reinforcement, reached the peak point and deformed until failure without significant degradation of lateral load carrying capacity. The ultimate failure was caused by crushing of confined concrete and buckling of longitudinal reinforcement of the compression zone. BC40 and BC80 showed no degradation of load carrying capacity until the failure while NC40 and NC80 showed some degradation after reaching peak load due to crushing of core concrete.

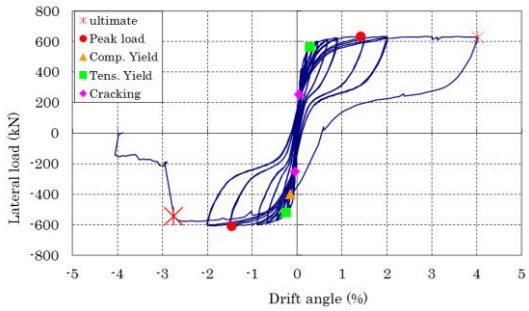

(a) BC40

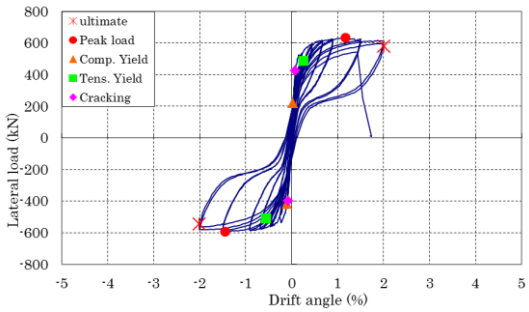

(b) BC80

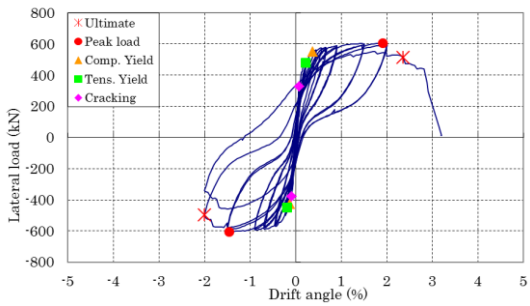

(c) NC40

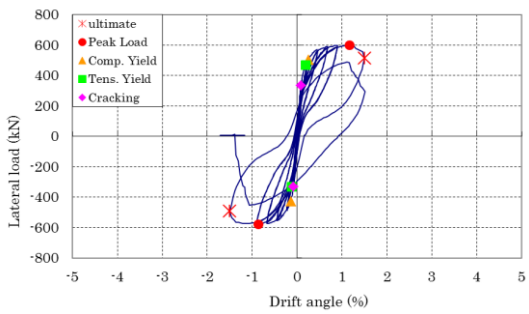

(d) NC80

Fig. 2 Experimental lateral load - drift angle relation

Fig. 3 shows crack patterns at the final cycle. Red and blue lines represent cracks in positive and negative directions, respectively. NC40 and NC80 have flexure-shear cracks which are basically continuous. Although BC40 and BC80 have flexure-shear cracks, flexural cracks and shear cracks are not necessarily continuous at the column interface. At the final stage, the failure was brittle because of core concrete crushing. Crushing happened only at the boundary column for BC40 and BC80. However, crushing of concrete extended to the center of the wall panel for NC40 and NC80 and wall panels buckled at the compression region as was seen for the 2010 Chile earthquake [4]. Buckling of longitudinal reinforcement at compression region was observed for all specimens but pulling out of reinforcement in the tensile region was not observed.

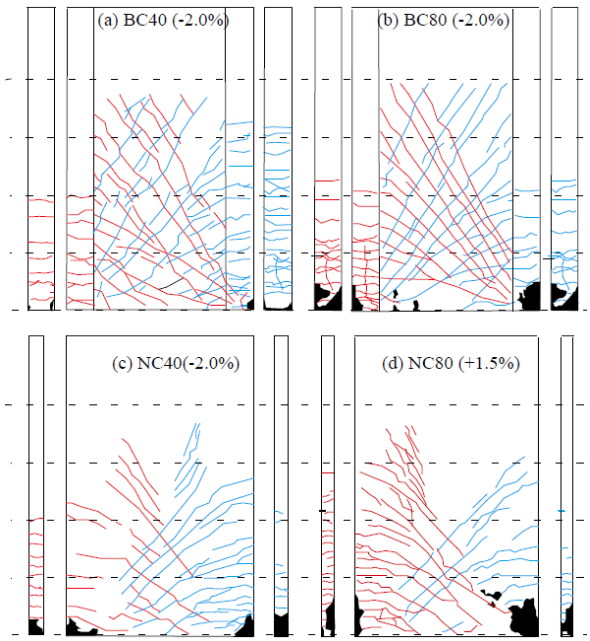

Fig. 3 Crack patterns at peak load

3. NONLINAR FINITE ELEMENT ANALYSIS

3.1. Finite element modeling

In order to simulate the behaviour of the tested RC walls, a numerical analysis was carried out using a 2-Dimentional finite element model. The FEM nonlinear analysis software FINAL [5] was used. Fig. 4 shows the FE mesh of BC40/BC80 specimens. Four-node quadrilateral isoparametric plane stress elements were used for concrete. The element size in the wall and the boundary regions was about 100 mmx100 mm. The foundation and loading beams were assumed to behave elastically. All nodes at the bottom of the foundation beam were pin-supported to restrain vertical and lateral displacement. The constant axial loads on the top of boundary regions were applied in the first step, and then the lateral load was applied at the loading beam center point under displacement control. Both monotonic and cyclic nonlinear analysis was conducted to simulate the load-deflection relation and predict the damage distribution.

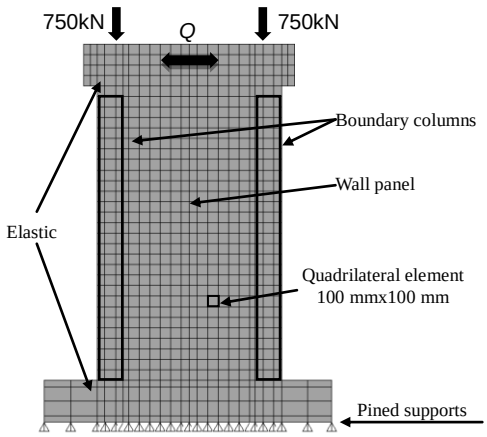

Fig. 4 FE mesh for BC40/BC80 specimens

3.2. Material constitutive laws

Mechanical properties of material used in the analysis are thus given in Table 2. The modified Ahmad model for the compressive stress-strain relationship of concrete was used [6]. The stress-strain curves follow Eq. 1 for both ascending and descending parts.

$$\sigma = \frac{\left[A.X + (D-1).X^2\right]\sigma_P}{1+(A-2)X + D.X^2} \tag{1}$$

with,

$$A = E_0 / E_P \tag{2}$$

$$X = \begin{cases} \varepsilon/\varepsilon_p & \text{for} \quad |\varepsilon| < |\varepsilon_p| \\ (\varepsilon/\varepsilon_p)^n & \text{for} \quad |\varepsilon| \geq |\varepsilon_p| \end{cases} \tag{3}$$

$$D = \begin{cases} \dfrac{19.6}{\sigma_B}\left(\dfrac{E_B}{E_P} - 1\right)^2 & \text{for} \quad |\varepsilon| < |\varepsilon_p| \\ 1 + \dfrac{177}{\sigma_B}\left(\dfrac{\sigma_P}{\sigma_B} - 1\right) & \text{for} \quad |\varepsilon| \geq |\varepsilon_p| \end{cases} \tag{4}$$

$$n = 1 + \frac{177}{\sigma_B}\left(\frac{\sigma_P}{\sigma_B} - 1\right) \tag{5}$$

where,

σ_P and ε_P: stress and strain at the peak point under multi axial stress, respectively

σ_B: uniaxial compressive strength

E_0: the elastic modulus

E_B and E_P: secant moduli corresponding to σ_P and σ_B, respectively.

The Kupfer-Gerstle's failure criterion was adopted for failure in biaxial compression and in tension-compression [7]. The modified Ahmad model was used for compression softening effect [8] with no strain softening at compressive strength after cracking. The strain at compressive strength is given by Eq. 6 [9].

$$\varepsilon_P = 1.37\sigma_P + 1690 \times 10^{-6} (\text{kgf/cm}^2) \tag{6}$$

The Naganuma model was adopted for concrete tension stiffing [6]. Uniaxial tensile strength is used for judging cracks under uniaxial and biaxial tension. Stress-strain relationship is assumed to be linear up to cracking. The tension stiffening after cracking is modeled as shown in Fig. 5.

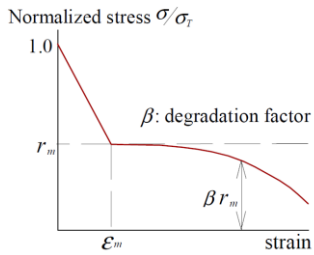

Fig. 5 Tension stiffening model of concrete [6]

The stress and strain at transition point are given as:

$$\varepsilon_m = 0.0016 - 0.024 p_s \tag{7}$$

$$\sigma_m = r_m \sigma_T = (0.6 - \sigma_B/177).\sigma_T \tag{8}$$

where,

σ_T: tensile strength

p_s: reinforcement ratio

β: degradation factor ($=E_c/E_0$)

E_c: tangential stiffness along the crack direction

The smeared crack model with a fixed angle concept was used to express cracking of concrete. The shear transfer model after cracks proposed by Naganuma was adopted [10]. For reinforcement material, the von Mises yield surface is employed to judge yielding under multi axial stress field along with the associated flow rule for isotropic hardening. The stress-strain relationship follows Ciampi's model [11] as shown in Fig. 6. All Horizontal and vertical reinforcements were smeared assuming a perfect bond. Interface elements between wall panel and foundation were not considered in this study.

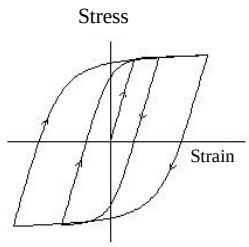

Fig. 6 Reinforcement material model [11]

3.3. Analysis results

Fig. 7 shows lateral load-drift angle relationships obtained analytically and experimentally. Both monotonic and cyclic analytical relations are plotted. Tables 3, 4 and 5 compare characteristic points: flexural cracking, yielding and peak load, respectively, derived from experiment and monotonic analysis for both positive and negative loading direction. The results show that the model is capable of simulating the entire steps of the nonlinear behaviour of the concrete wall such as elastic region, cracking, steel yielding and peak load with good accuracy. Simulation of specimens BC40 and BC80 under monotonic loading shows a nonlinear flexural behaviour in good agreement with

the experiment since the model was able to simulate the ductile behavior up to drift angle of 1.5% quite well with a slight overestimation of the peak load. For specimens NC40 and NC80, the model didn't simulate well their flexural behavior after reaching the peak load, since the strength dropped after 0.5% drift angle. This is due the high level of axial load, and to the confinement effect that the 2-D model could not explicitly take into account for walls without boundary columns when compared to a 3-D model.

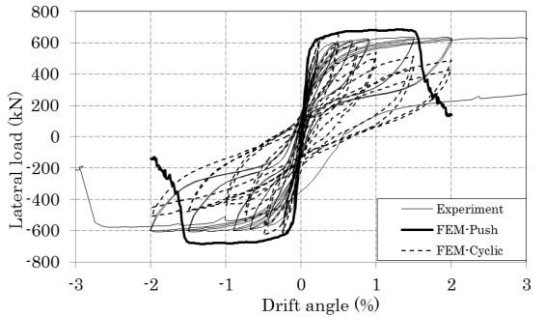

(a) BC40

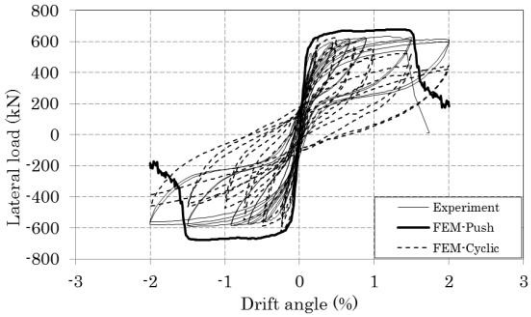

(b) BC80

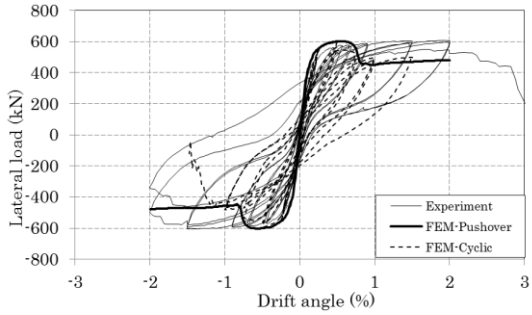

(c) NC40

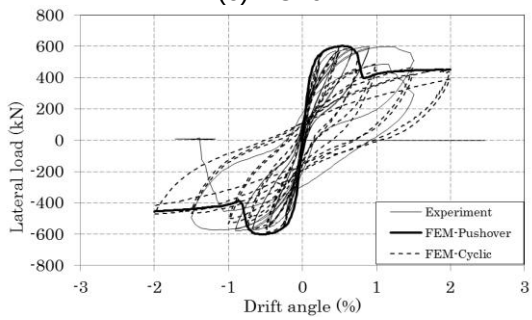

(d) NC80

Fig. 7 Experimental and FEM lateral load - drift angle relations

Cyclic analysis lateral load-drift angle relationships show a good agreement up to 0.75% drift angle with a drop of performance beyond that for all specimens. This is probably because the model overestimates the damage accumulation after this level of drift angle which contribute to strength reduction. It is also noted that cyclic analysis overestimated residual deformations after 0.75% drift angle compared to experimental hysteresis curves that had very small residual drift at most cycles. Small residual drift is probably due to high concrete strength and axial force which made specimens behave like post-tensioned precast concrete structures.

Fig. 8 shows cracks distribution and damage pattern at 1.5% drift angle under monotonic loading analysis for positive loading direction. For walls with boundary columns, the crack distribution was less spread in the case of walls with boundary elements compared to that of rectangular walls. Damage for walls with boudary column is concentrated at the outside bottom of boundary columns, while for walls without boundary damage extended along the bottom of confined regions. This is due to the fact that boundary columns carry a large amount of axial force to reduce axial stress level of wall panels to reduce their damage.

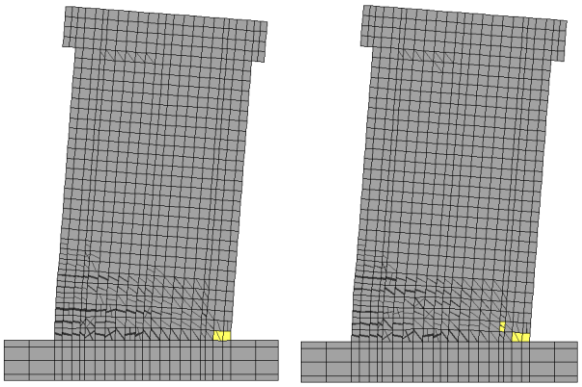

(a) BC40 (b) BC80

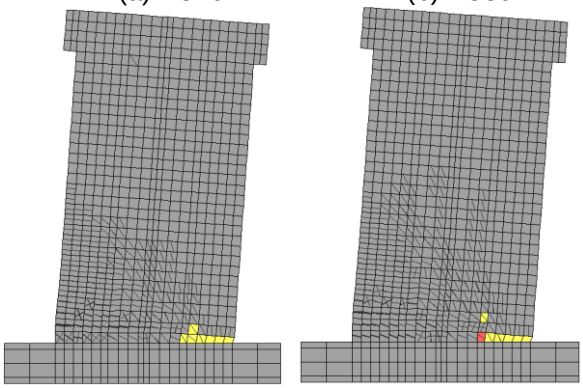

(c) NC40 (d) NC80

Fig. 8 Damage pattern at 1.5% drift angle

Table 3 Comparison of flexural cracking point

	Experiment		Analysis	
	R (%) (+)/(-)	Q (kN) (+)/(-)	R (%)	Q (kN)
BC40	0.05/-0.05	253/-253	0.06	346
BC80	0.08/-0.06	424/-400	0.07	400
NC40	0.07/-0.09	328/-379	0.05	231
NC80	0.08/-0.07	334/-331	0.05	231

Table 4 Comparison of steel yielding point

	Experiment		Analysis	
	R (%) (+)/(-)	Q (kN) (+)/(-)	R (%)	Q (kN)
BC40	0.29/-0.25	562/-521	0.11	546
BC80	0.03/-0.09	219/-417	0.11	546
NC40	0.23/-0.20	478/-449	0.17	505
NC80	0.19/-0.11	467/-332	0.17	505

Table 5 Comparison of peak load point

	Experiment		Analysis	
	R (%) (+)/(-)	Q (kN) (+)/(-)	R (%)	Q (kN)
BC40	1.41/-1.47	634/-607	1.48	675
BC80	1.17/-1.45	633/-592	1.09	677
NC40	1.91/-1.46	606/-605	0.57	602
NC80	1.16/-0.87	598/-578	0.51	601

4. CONCLUSIONS

Nonlinear finite element analyses were conducted on four cantilever type structural RC walls with and without boundary columns with different amount of shear reinforcement in the confined regions. The following conclusions can be drawn.

(1) The built FE model was able to simulate the entire steps of the nonlinear behaviour of the concrete wall such as elastic region, cracking, steel yielding and peak load with good accuracy. The model was also able to simulate the flexural behaviour of walls with boundary columns under monotonic loading.

(2) The built model predicted damage pattern quite well, and has pridicted the ability of boundary columns in reducing damage level and crack distribution since boundary columns carry a large amount of axial force which reduce axial stress level in wall panels. In this manner, boundary columns can contribute effectivelly in preventing failure mode due to wall buckling especially when subjected to high axial load.

(3) Under cyclic loading, the model overestimated residual deformations after 0.75% drift angle compared to experimental hysteresis curves.

(4) The current study presents an intermediate step where 2D models were created to study the overall behavior with mainly focusing on the maximum strength. For future detailed modeling and analysis of the behavior and observed damage, the 3D modeling will be used to take width effects into account and to apprehend more accurately deformability of the walls.

ACKNOWLEDGEMENT

This research work was financially supported by the Ministry of Land, Infrastructure, Transportation and Tourism. The support of Dr. H. Fukuyama is also acknowledged. The authors wish also to acknowledge the anonymous reviewer for his/her detailed and helpful comments to the manuscript.

REFERENCES

[1] Zhang, H., Lu X. and Wu, X., “Experimental Study and Numerical Simulation of the Reinforced Concrete Walls with Different Stirrup in the Boundary Element”, Journal of Asian Architecture and Building Engineering, Vol.9 No.2, Nov. 2010, pp. 447-454.

[2] Oh, Y. H., Han, S. W. and Choi, Y. W., “Evaluation and Improvement of Deformation Capacities of Shear Walls Using Displacement-Based Seismic Design”, International Journal of Concrete Structures and Materials, Vol.18, No.1E, Jun. 2006, pp. 55-61.

[3] Sakamoto, K., Sakashita, M., Kono, S. and Tani, M., “Effects of boundary columns on the Ultimate Flexural Deformation of Cantilever Structural Walls”, 2012 JCI Convention Proceedings, Vol.34, No.2, 2012, pp. 379-384. (in Japanese)

[4] Naeim, F., Lew, M., Carpenter, L. D., Youssef, N. F., Rojas, F., Saragoni, G. R. and Adaros, M. S., “Performance of tall buildings in Santiago, Chile during the 27 February 2010 offshore Maule, Chile earthquake”, The Structural Design of Tall and Special Buildings, 2011, 20(1): 1–16.

[5] ITOCHU Techno-solutions Corportation, FINAL/V11 Help.

[6] Naganuma, K., Yonezawa, K., Kurimoto, O., Eto, H., “Simulation of nonlinear Dynamic response of Reinforced Concrete Scaled Model Using Three-Dimentional Finite Element Method”, 13th WCEE Proceedings, Vancouver, B.C., Canada, Aug. 1-6, 2004, Paper No 586.

[7] Kupfer, H. B. and Gerstle, K. H., Behavior of Concrete under Biaxial Stress, ASCE J. Eng. Mech. Div., 99(EM4), 1973, pp. 853-866.

[8] Naganuma, K., “Stress-strain Relationship of Concrete under Triaxial Compression”, Journal of Structural and Construction Engineering, AIJ, No. 474, Aug. 1995, pp. 163-170. (in Japanese)

[9] Amemiya, A. and Noguchi, H., “Development of Finite Element Analysis Program for High Strength Reinforced Concrete Members (Development of Concrete Model, Part 1)”, Summaries of Technical Papers of Annual Meeting, AIJ, Sep., 1990, pp. 639-640. (in Japanese)

[10] Naganuma, K., “Nonlinear Analytical Model for Reinforced Concrete Panels under In-Plane Stresses”, J. Struct. Constr. Eng. Trans. AIJ, No.421, 1991, pp. 39-48. (in Japanese)

[11] Ciampi, V., Eligehausen R., Bertero V. V., Popov E. P., “Analytical model for concrete anchorages of reinforcing bars under generalized excitations”, Report No. UCB/EERC82-23, EERC, Berkeley, California, 1982.